



## EFFECT OF INTERFACIAL RESISTANCE OF SUPERCONDUCTING-STABILIZER LAYER ON THE NORMAL ZONE PROPAGATION VELOCITY FOR 2G HTS TAPES

Gladya Anusha. A<sup>1</sup>, S. Ajin Sundar<sup>2</sup>

<sup>1,2</sup>Department of Physics, St. Jude's College, Thoothoor, Affiliated to Manonmaniam Sundaranar University, Tirunelveli, India

### Abstract

High temperature superconducting (HTS) tapes of the second generation have been widely used as energy storage materials, such as in superconducting magnetic energy storage (SMES) devices. In order to enhance the current-carrying characteristics, these systems are typically run close to the critical currents of the coated conductors; as a result, hot spots may develop, which could cause the superconductor to become quenched. In order to prevent the start of hot spots and to reduce the amount of faulting, efforts have been made to raise the normal zone propagation velocity (NZPV) in this manuscript. The interfacial resistance between the superconductor and stabilizer layer, which can act as a current flow diverter during fault circumstances, has been shown to be the key to producing massive NZPV. The architecture of the tape has been somewhat modified by the addition of a high resistive layer between the superconducting and stabilizer layers, where various interfacial resistances have been used to predict the temperature distribution between HTS tape with a length of 10 cm. A 2D numerical model has been developed using COMSOL to evaluate the NZPV and temperature distribution among the 2G superconducting tape. It has been concluded that higher NZPVs can be achieved with large interfacial resistances through which quenching of superconducting tape can be prevented.

**Keywords:** HTS tape, normal zone propagation velocity, interfacial resistance, quench, HTS cables, SFCL, SMES.

### 1. Introduction

Coated conductors are extensively used for power applications due to their capability to carry large currents and work efficiently near the critical currents. Almost in all power applications like cables, motors, generators, transformers, MRIs, NMRs, fault current limiters and SMES systems coated conductors have replaced copper conductors as they are more efficient in handling currents and need less space than conventional devices. As fault current limiting and energy storage devices work near the critical currents so there may be situation arises when hot spots may come into existence which may lead to quench of the superconductor. The development of HTS cables is also receiving attention these days where design of current carrying cable is done with higher load factors (near critical currents) in order to maximize its current carrying capacity. However, large currents can create unbalance due to heat generation and due to inefficient cooling it may lead to hot spots and further to the thermal quench of the tape. This issue is still to be addressed and many research groups are working on this aspect

theoretically/computer modeling [1]–[8] and experimentally [9][10].

When a current, ' $I$ ' is applied to such devices is found to near critical current  $I_c$  then there may be some locations where hot spots (due to thermal instabilities) may appear in the weaker zones of the superconducting tape. Inhomogeneities in the materials like superconducting tape can be arises due to manufacturing defects at micro-scale that can affect the  $I_c$  of the tape or any other phenomena such as existence of external magnetic field results into the arbitrary increase in the temperature of the superconducting tape locally which further leads to hot spots. Such hot spots can damage the whole systems if local temperature exceeds the critical value. Thus, it becomes essential to avoid hot spots among the superconductors used for any application in order to prevent the failure of the system.

Quenching is a phenomenon when temperature of superconducting tape exceeds critical value and as discussed earlier it may arise due to hot spots. Hot spot concerns subsist in all superconducting devices however they are more prominent in SMESs and SFCLs systems as in the former, the operating currents are usually chosen as close as to  $I_c$  to maximize the field generated [11] and in the later, its primary method of operation relies on superconductor quenching [12][13]. Studies reveal that for coated conductors NZPVs are low, this makes them susceptible to hot spots and this result into the drastic increase in the temperature before enough voltage drop appears and detecting the quench in instance of superconducting magnets [14][15], cables [16][17] or SFCLs [18]–[22].

Various strategies have been adopted to mitigate hot spot challenges and amongst them, extending the thickness of the stabilizer or substrate layer is frequently utilized to enhance the thermal mass. [23]. Though, only over-sizing the tape by increasing copper's thickness not serves the purpose and a marginal current (temperature) is required to provide the enough time before the detection of the quench and to modify or stop the input current before the system failure. Therefore, it is better to work near 80% of load factor which provide enough margins to take care such issues. However, this margin obviously reduces the current carrying capacity of cable or maximum attainable magnetic field inside the magnet [11].

Increase NZPV as a second strategy to reduce temperature rise at hot locations; however, it reduces the stability margin of the superconducting tape. This factor can be enumerated by the minimum energy required to initiate a quench and this energy is generally known as minimum quench energy (MQE) [24], [25]. Numerous methods have been proposed by various researchers in order to enhance the NZPV in the coated conductors. For illustration, researchers have suggested to use sapphire as a substitute for Hastelloy whose electrical and thermal properties favors large NZPV [26]. Recently, researchers have suggested to intentionally increasing the interfacial resistance among the stabilizer and superconductor to enhance the NZPV in coated conductors [27]–[29]. This escalate the current transfer length (CTL) among stabilizer and superconductor. This concept is easy to implement and provides attractive solutions, however, the critical challenges exist in increasing the interfacial resistance is associated with the amount of heat generation at the interface of current leads connections as at this location the temperature increased drastically such that it may cause quenching of the superconductor.

In this work, keeping large interfacial resistances, simple superconducting tape architecture has been used to increase NZPV. Here it has been assumed that Along the breadth of the tape, the interfacial resistance varies, instead having a segment of very low interfacial resistance and the

other segment with very high interfacial resistance. A 2D numerical model has been developed using Comsol MultiPhysics and a comparison has been made for NZPV among different interfacial resistances.

## 2. Numerical Modelling

2D model has been developed in the Comsol MultiPhysics 5.4 where Joule heating module has been employed for the numerical solution of the model. Electro-thermal behavior of the coated conductor has been examined where interfacial resistance amongst the superconducting and stabilizer layer has been varied. The basic geometry and methodology followed has been explained in the following sections.

### 2.1 Geometrical details

Coated conductors have been used for the present study whose geometry is given in Figure 1 where length of the tape assumed to be 10 mm and other parameters are tabulated in Table 1. The width of the tape is 12 mm and the thickness of superconducting (SC) layer is 1  $\mu\text{m}$ . Generally, SC tape consists of four layers viz; stabilizer, superconducting layer, substrate and buffer layers. For the tape that has been assumed in the present study, the stabilizer layer is composed as silver (Ag), superconducting layer as ReBaCuO, substrate as Hastelloy and buffer layer using MgO. The architecture of the tape has been given in Figure 2 where longitudinal arrangement of the different layers has been presented. The marked arrows represent the virtual probe locations which are generally used to evaluate the electric field variations with time those are separated by a distance of 1 mm. Multi-colors are used to distinguish the different layers and Figure 2 represents that from left end current has been supplied and the other end is grounded which consists low  $J_c$  region at the end of the superconducting tape. The highly resistive layer can be termed as current flow diverter as it is responsible for diverting the current from SC region to stabilizer in order to ensure the safety of the superconducting tape from quenching. most of the tape's temperature dependent properties has been taken from [23-28]. A detailed information is available on the properties like thermal conductivity, specific heat and electrical resistivity/conductivity of buffer layer (MgO), stabilizer (Ag), Substrate (Hastelloy) and SC tape (ReBCO for  $T > T_c$ ) is present in [30]–[35]. As the tape is required to cool at 77 K thus all property data is extracted on this liquid nitrogen temperature.

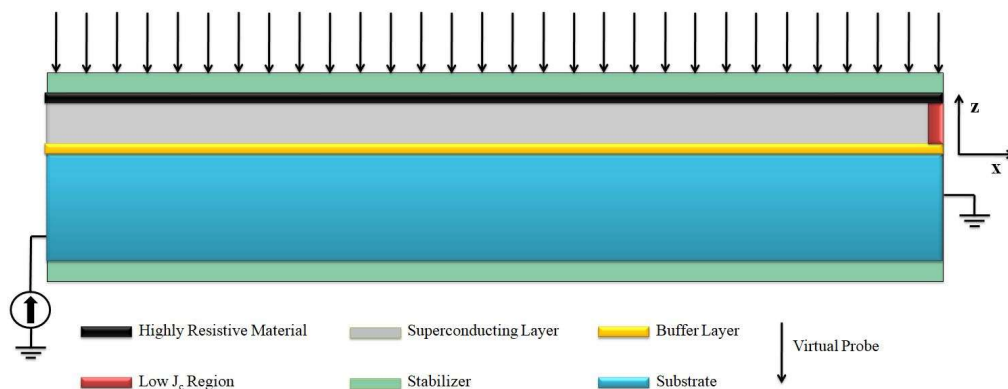


**Figure 1 Tape Architecture**

A mathematical model with few modifications has been used as that of Lacroix et al [8] in the present study, current densities are considered 100 times greater than that of Lacroix model and the tape width is considered to be 12 mm instead of 4 mm. Also, authors have not studied

how the NZPV is affected by different interfacial resistance which has been done in this work. Due to the non-linear behavior of resistivity below  $T_c$ , electrical conductivity is also behaving in the similar way thus power-law model is used to approximate the electrical conductivity of (Re)BaCuO in the flux creep and flux flow regions ( $\sigma_{sc}$ ). However, the electrical conductivity of normal state while transition from superconducting state can be modelled by taking into account two parallel resistances. The subsequent expressions have been used for the present simulations:

$$\sigma_{sc}(T) = \frac{J_c(T)}{E_0} \left( \frac{\|E\|}{E_0} \right)^{\frac{1-n(T)}{n(T)}} \quad (1)$$

$$J_c(T) = \begin{cases} J_{c0} \left( \frac{T_c - T}{T_c - T_0} \right) & \text{for } T < T_c \\ 0 & \text{for } T_c \leq T \end{cases} \quad (2)$$

$$n(T) = \begin{cases} (n_0 - 1) \left( \frac{T_c - T}{T_c - T_0} \right)^{1/4} + 1 & \text{for } T < T_c \\ 1 & \text{for } T_c \leq T \end{cases} \quad (3)$$

**Table 1 Nomenclature**

$J_{c0}$	Critical current density at $T_0$
$T_0$	Liquid nitrogen temperature
$\ E\ $	Norm electric field
$T_c$	Critical temperature
$n_0$	Fitting parameter
$d$	Width of the low $J_c$ region
$A$	Amplitude of the low $J_c$ region
$l$	Position of the low $J_c$ region
$I(t)$	Applied transport current
$\Omega$	Represents the surface at one end of the tape
$\mathbf{n}$	Local unit vector perpendicular to the external surfaces of the tape
$\sigma(T)$	Electrical conductivity
$\rho_m$	Mass density of the tape
$C_p(T)$	Heat capacity
$k(T)$	Thermal conductivity

## 2.2 Electro-thermal modelling

For the purpose of starting the normal zone propagation, a low  $J_c$  region has been incorporated in the tape architecture highlighted by red area as mentioned in Figure 1. Same model as that of Lacroix et al [8] has been imitated in the present study as shown in Figure 2 where reduction in the critical current has considered by the following relation:

$$J_{c0} \rightarrow J_{c0} \left[ 1 - Ae^{-\frac{(x-l)^2}{2d^2}} \right] \quad (4)$$

It has been designed in such a way that whenever current density through the superconducting tape exceeded  $J_{c0}(1 - A)$  then heat is generated at low  $J_c$  region which further generates normal zone and that is expected to expand with time. Potential  $V$  and the temperature  $T$  are the variables for the electro-thermal model of the superconducting tape. The governing equations used for electro-thermal modelling are as follows:

**Electrical part**

$$\nabla \cdot (-\sigma(T)\nabla V) = 0 \quad \text{within the tape} \quad (5)$$

$$\int_{\Omega} -\mathbf{n} \cdot (-\sigma(T)\nabla V) dS = I(t) \quad \text{at left end of the tape} \quad (6)$$

$$V = 0 \quad \text{at the other end of the tape} \quad (7)$$

$$\mathbf{n} \cdot \nabla V = 0 \quad \text{at the remaining boundaries of the tape} \quad (8)$$

**Thermal part**

For the thermal analysis, heat equation can be written as

$$\rho_m C_p(T) \frac{\partial T}{\partial t} + \nabla \cdot (-k(T)\nabla T) = Q_j \quad \text{in the tape} \quad (9)$$

Joule heating losses can be evaluated using following coupled correlation:

$$Q_j = \sigma(T)(-\nabla V)^2 \quad \text{in the tape} \quad (10)$$

For the present study, it has been assumed that the temperature gradient at the both ends of the tape is zero as described by following equation:

$$\mathbf{n} \cdot \nabla T = 0 \quad \text{at the both ends of the tape} \quad (11)$$

Regarding the remaining boundaries, as superconducting tape is assumed to be through liquid nitrogen at 77 K therefore, the cooling power required by the nitrogen can be evaluated through the following relation:

$$\mathbf{n} \cdot (k\nabla T) = h(T - T_0) \quad \text{at the remaining boundaries} \quad (12)$$

**2.3 Numerical Approximations**

For the 2D analysis, infinitely thin domains are used to represent buffer layers and interfacial resistance layers which further implies that in-plane ( $J_x$  and  $J_y$ ) current densities are taken as negligible and only normal component of current density ( $J_z$ ) has been considered. Therefore, after such approximations (6) becomes:

$$J_z = \sigma(T) \frac{\partial V}{\partial z} = \sigma(T) \left( \frac{V_2 - V_1}{t} \right) \quad (13)$$

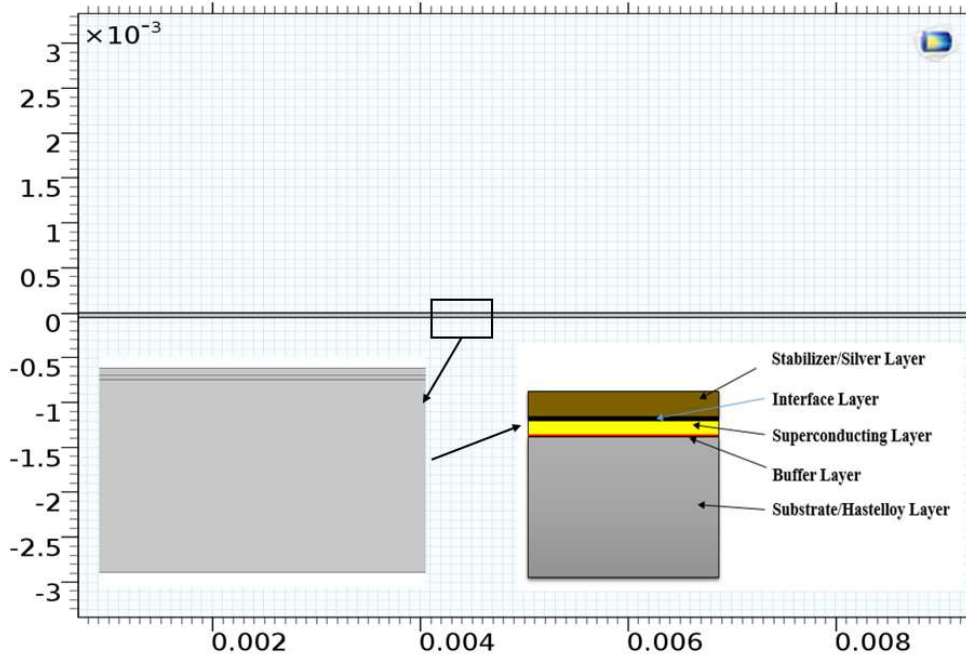


Figure 2 Electro-thermal model details

The potentials on either side of the infinitely thin layer are  $V_2$  and  $V_1$ , and the layer's thickness is  $t$ . Similarly, the heat flux ( $Q_z$ ) circulating across multiple tiny layers can be calculated using following equation:

$$Q_z = k(T) \frac{\partial T_1}{\partial z} = k(T) \left( \frac{T_2 - T_1}{t} \right) \quad (14)$$

Table 2 Modelling Parameters involved in quench analysis

Parameter	Numerical Value
Length	10 cm
Width	12 mm
Substrate thickness	50 $\mu\text{m}$
Buffer layer thickness	150 nm
Superconducting layer thickness	1 $\mu\text{m}$
Interfacial layer between superconductor and stabilizer thickness	100 nm
Current flow diverter thickness	100 nm
Stabilizer thickness- top	2 $\mu\text{m}$
Stabilizer thickness- sides and bottom	1 $\mu\text{m}$
Substrate thickness	50 $\mu\text{m}$

The temperatures on either side of the infinitely thin layer are  $T_2$  and  $T_1$ , respectively, and the layer's thermal conductivity is  $k(T)$ . Lacroix et al [8] found that in the infinitely thin layer, both electric potentials and temperatures are discontinuous for such approximations and on the two sides of the layer, the potential and temperature values differ. Interface boundary conditions

(13) and (14) can be used to manage this value shift. which is a representation of the lumped approximation in continuous case and this significantly depends upon thin layer material properties i.e. electrical conductivity, thermal conductivity and thickness of the layer.

### 3. Mesh Sensitivity Studies

The computational domain is discretized with mapped meshing where each layer of the superconducting tape including stabilizer, substrate and superconducting layer is sub-divided into small sub-domains using mapped meshing technique. Superconducting tape of 10 cm length is discretized in transverse direction using 100, 200, 300, 400 and 500 elements as shown in Figure 3. It can be observed from Table 3 that for case-3, the maximum temperature rise within the tape for electrical conductivity  $1e9$  S/m is equal to case-4 and case-5. However, the computational time elapsed for analysis and degree of freedoms for case-3 are found to less thus this meshing has been used for rest of the studies. The system configurations were as follows: Intel Core i5-8250 CPU @1.6GHz, 8GB RAM, 64-bit operating system with Window 10.

**Table 3 Mesh sensitivity studies for electro-thermal analysis of the HTS tape**

Sr. No.	Number of elements	Number of domain elements	Number of domain boundaries	Degree of freedom	Time (s)	Max. Temp. (K)
1.	100	3000	460	25327	22m 56s	95
2.	200	6000	860	50527	42m 47s	94.9
3.	300	9000	1260	75727	1h 4m 37s	94.7
4.	400	12000	1660	100927	1h 48m 32s	94.7
5.	500	15000	2060	126127	1h 56m 39s	94.7

Figure 3 (a) shows that there is one partition till 0.1 mm length of the SC tape and 5 partitions can be noticed in Figure 3 (e). However, Figure 3 (c) has been selected for the further studies due to the mesh density saturation has been found above this value.

### 4. Results and Summary

The parameters involved in the quench dynamics are tabulated in the Table 2 where 2G HTS coated conductors have been tested for various interfacial resistance amid the superconducting and stabilizer layer. For the modelling purposes, electrical conductivity has been used as input material property instead of resistivity. The right end of the tape is grounded and the effect of this has been tested for various electrical conductivities of the interface. More NZPV is required which implies the information regarding the fault has to dispersed uniformly to the left end so that uniform temperature distribution can be obtained in order to avoid instant gradients.

To evaluate the consequence of interfacial resistance on the normal zone propagation velocity, a 2D model of a straight superconductor having length 10 cm has been drawn in Figure 1. Table 4 represents the different NZPVs achieved for various electrical conductivity input. To evaluate

the NZPV, distance among the probes (shown in Figure 1) i.e. 1 mm is divided with the time elapsed to reach the same temperature as shown in Figure 4 and (15).

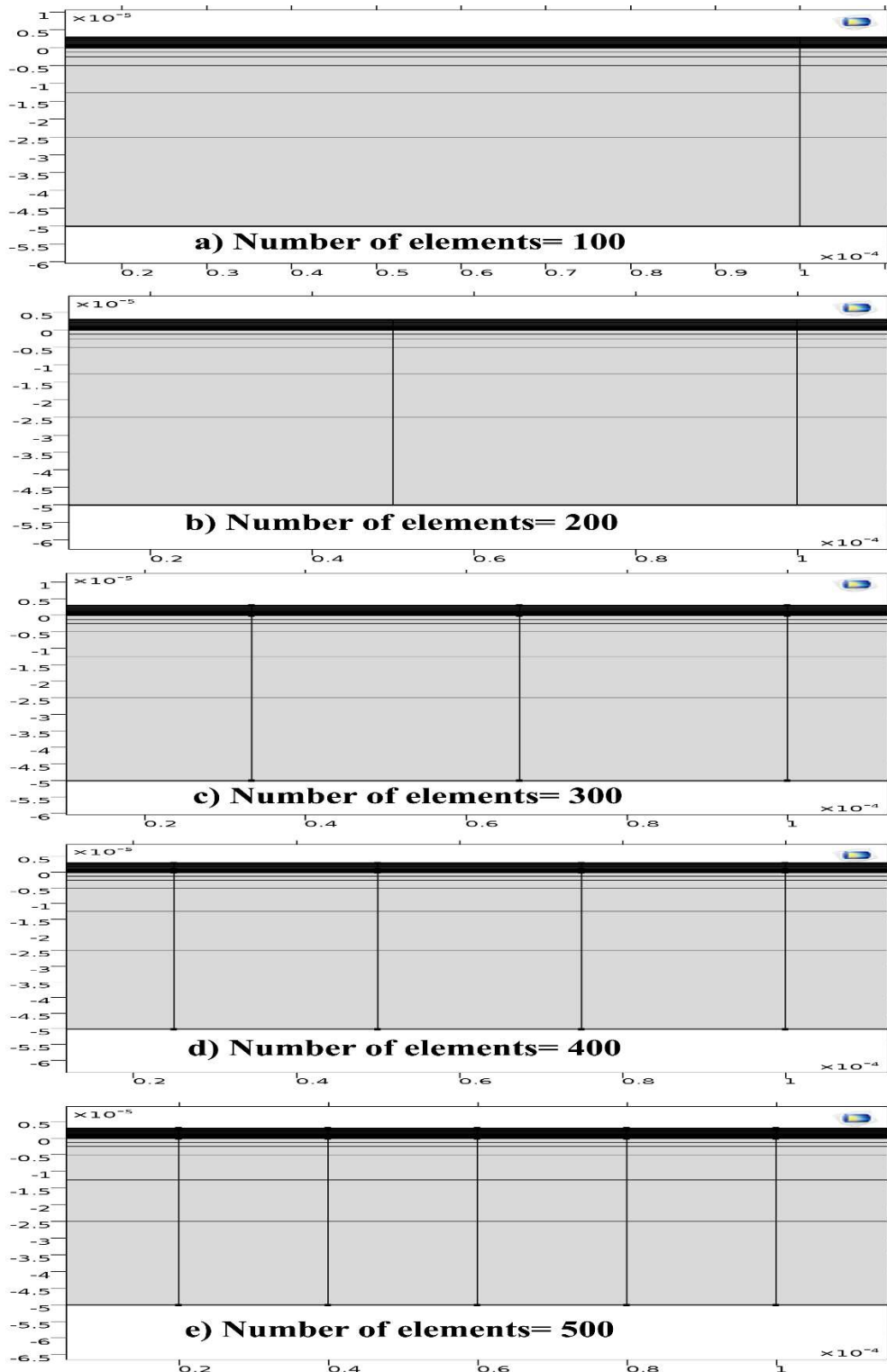


Figure 3 Mesh density analysis for 0.1 mm length of tape (a) 1 partition, (b) 2 partitions, (c) 3 partitions, (d) 4 partitions and (e) 5 partitions.



$$\text{Normal zone propagation velocity} = \frac{1}{\text{Time elapsed}} \quad (15)$$

**Table 4 Normal Zone Propagation Velocity for various electrical conductivity**

Electrical Conductivity (S/m)	NZPV (cm/s)
1e9	63.69
1e7	90.9
1e5	153.84
1e3	256.4
1e1	312.5
1e0	666.67

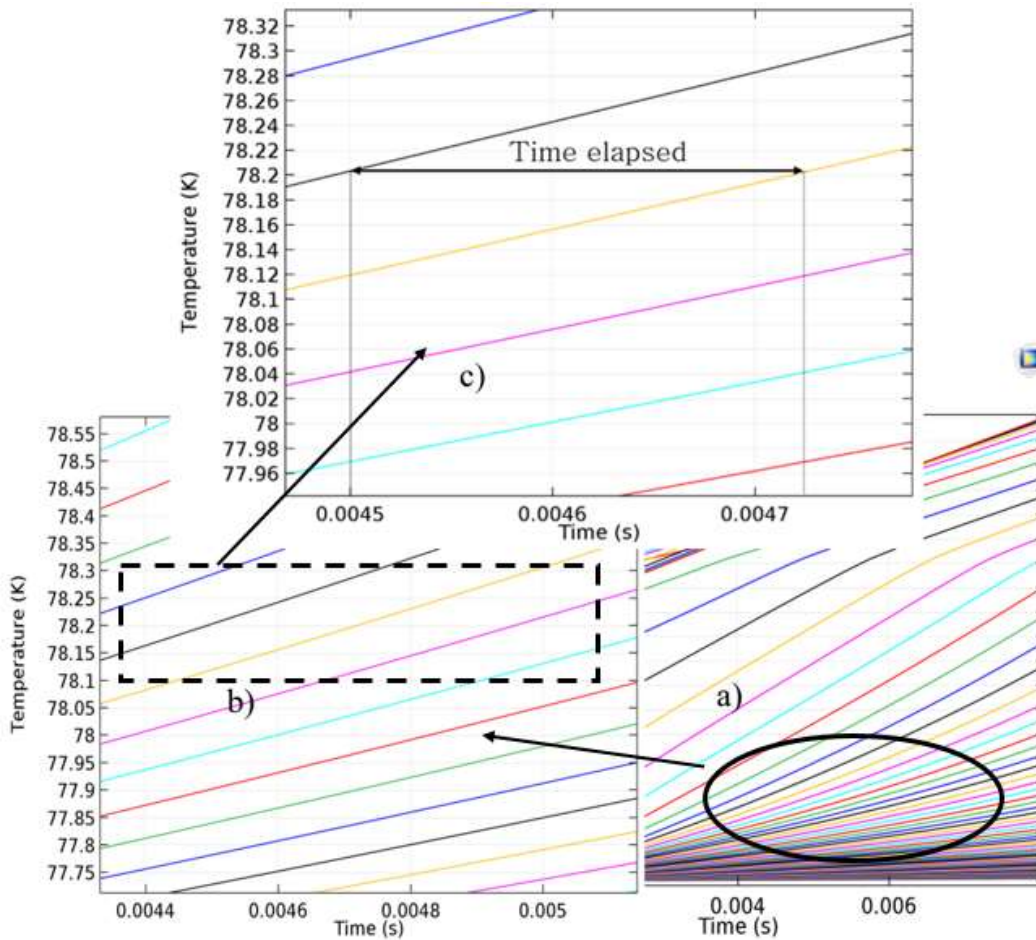


**Figure 4 Temperature plot vs time**

**EFFECT OF INTERFACIAL RESISTANCE OF SUPERCONDUCTING-STABILIZER LAYER ON THE NORMAL ZONE PROPAGATION VELOCITY FOR 2G HTS TAPES**

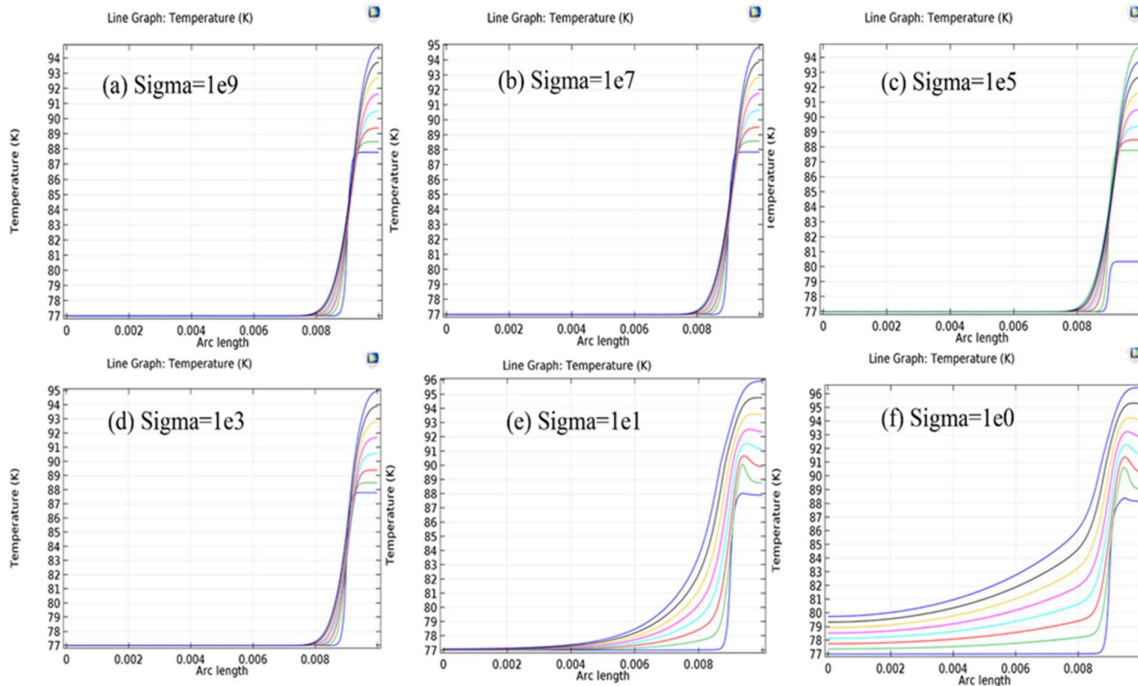


**Figure 5 Temperature plot for various time steps and electrical conductivity**

Figure 5 illustrate the temperature plots for different time steps and electrical conductivity and it can clearly visualize that with the increase in the interfacial resistance (from Figure 5 (a) to Figure 5 (f)), the NZPV is found to increase (Table 4). Further, it can be observed that the temperature gradient is found to less for higher resistances (Figure 5 (f)) compared to lower (Figure 5 (a)). Thus, it has been concluded that higher interfacial resistances can increase the NZPV of the fault detection. It can further help in identifying the exact location of the fault.

### 5. Conclusions

From the electro-thermal analysis of the superconducting tape, it has been concluded that with the increase in the interfacial resistance of the superconducting-stabilizer layer, the NZPV can be enhanced and which can assist in controlling the quenching of the tape. It has been found from the study that a NZPV of 666.67 cm/s can be achieved for an electrical conductivity of 1 S/m. This study will be helpful in understanding the quench protection systems and how this NZPV can affect the HTS coated conductor tape protection unit.

### References

- [1] Y. Tong, M. Guan, and X. Wang, "Theoretical estimation of quench occurrence and propagation based on generalized thermoelasticity for LTS/HTS tapes triggered by a spot heater," *Supercond. Sci. Technol.*, vol. 30, no. 4, p. 45002, 2017.
- [2] J. Nugteren, "Normal zone propagation in a YBCO superconducting tape: Measurement and analysis of quasi-adiabatic normal zone propagation in a YBCO coated conductor." University of Twente, 2012.
- [3] G. Escamez, C. Lorin, T. Wu, and P. J. Masson, "Quench propagation in ybco racetrack of a rotor winding," 2013.
- [4] T. Benkel, Y. Miyoshi, X. Chaud, A. Badel, and P. Tixador, "REBCO tape performance

- under high magnetic field,” *Eur. Phys. J. Appl. Phys.*, vol. 79, no. 3, p. 30601, 2017.
- [5] M. J. Wolf, R. Heller, W. H. Fietz, and K.-P. Weiss, “Design and analysis of HTS subsize-conductors for quench investigations towards future HTS fusion magnets,” *Cryogenics (Guildf)*, p. 102980, 2019.
- [6] X. Zhang *et al.*, “Active Quenching Technique for YBCO Tapes: Quench Acceleration and Protection,” *J. Supercond. Nov. Magn.*, vol. 31, no. 11, pp. 3465–3474, 2018.
- [7] Y. Wang, J. Zheng, Z. Zhu, M. Zhang, and W. Yuan, “Quench behavior of high temperature superconductor (RE)BCO CORC cable,” *J. Phys. D. Appl. Phys.*, 2019.
- [8] C. Lacroix and F. Sirois, “Concept of a current flow diverter for accelerating the normal zone propagation velocity in 2G HTS coated conductors,” *Supercond. Sci. Technol.*, vol. 27, no. 3, p. 35003, 2014.
- [9] L. Ren *et al.*, “Experimental Analysis of Quench Characteristic in HTS Tapes and Coils,” *IEEE Trans. Appl. Supercond.*, vol. 29, no. 5, pp. 1–6, 2019.
- [10] J. Pelegrín *et al.*, “Experimental and numerical analysis of quench propagation on MgB<sub>2</sub> tapes and pancake coils,” *Supercond. Sci. Technol.*, vol. 26, no. 4, p. 45002, 2013.
- [11] S. Awaji *et al.*, “Hot spot behavior of Y123 coated conductors,” *IEEE Trans. Appl. Supercond.*, vol. 22, no. 3, p. 6601004, 2011.
- [12] P. Tixador and N. T. Nguyen, “Design of ReBaCuO-coated conductors for FCL,” *Supercond. Sci. Technol.*, vol. 25, no. 1, p. 14009, 2011.
- [13] D. Colangelo and B. Dutoit, “Inhomogeneity effects in HTS coated conductors used as resistive FCLs in medium voltage grids,” *Supercond. Sci. Technol.*, vol. 25, no. 9, p. 95005, 2012.
- [14] X. Wang, U. P. Trociewitz, and J. Schwartz, “Self-field quench behaviour of YBa<sub>2</sub>Cu<sub>3</sub>O<sub>7- $\delta$</sub>  coated conductors with different stabilizers,” *Supercond. Sci. Technol.*, vol. 22, no. 8, p. 85005, 2009.
- [15] C. Marinucci, L. Bottura, M. Calvi, and R. Wesche, “Quench analysis of a high-current forced-flow HTS conductor model for fusion magnets,” *IEEE Trans. Appl. Supercond.*, vol. 21, no. 3, pp. 2445–2448, 2010.
- [16] M. Ichikawa, S. Torii, T. Takahashi, H. Suzuki, S. Mukoyama, and M. Yagi, “Quench properties of 500-m HTS power cable,” *IEEE Trans. Appl. Supercond.*, vol. 17, no. 2, pp. 1668–1671, 2007.
- [17] M. Marchevsky, Y. Y. Xie, and V. Selvamanickam, “Quench detection method for 2G HTS wire,” *Supercond. Sci. Technol.*, vol. 23, no. 3, p. 34016, 2010.
- [18] H. Kato, O. Miura, and D. Ito, “Quench behaviors of QMG current limiting elements under the influence of magnetic field,” *IEEE Trans. Appl. Supercond.*, vol. 10, no. 1, pp. 869–872, 2000.
- [19] S. Elschner, F. Breuer, H. Walter, and J. Bock, “Magnetic field assisted quench propagation as a new concept for resistive current limiting devices,” in *Journal of*

*Physics: Conference Series*, 2006, vol. 43, no. 1, p. 917.

- [20] B. Xiang *et al.*, “Effects of Magnetic Fields on Quench Characteristics of Superconducting Tape for Superconducting Fault Current Limiter,” *Appl. Sci.*, vol. 9, no. 7, p. 1466, 2019.
- [21] T. Matsumura, T. Uchii, and Y. Yokomizu, “Development of flux-lock-type fault current limiter with high-T/sub c/superconducting element,” *IEEE Trans. Appl. Supercond.*, vol. 7, no. 2, pp. 1001–1004, 1997.
- [22] B. W. Lee, K. B. Park, J. S. Kang, and I. S. Oh, “Quench characteristics of YBCO thin films using magnetic field source for superconducting fault current limiters,” *Prog. Supercond. Cryog.*, vol. 6, no. 2, pp. 11–14, 2004.
- [23] Y. Fu, O. Tsukamoto, and M. Furuse, “Copper stabilization of YBCO coated conductor for quench protection,” *IEEE Trans. Appl. Supercond.*, vol. 13, no. 2, pp. 1780–1783, 2003.
- [24] L. Dresner, *Stability of superconductors*. Springer Science & Business Media, 2006.
- [25] X. Wang, U. P. Trociewitz, and J. Schwartz, “Near-adiabatic quench experiments on short Y Ba 2 Cu 3 O 7–  $\delta$  coated conductors,” *J. Appl. Phys.*, vol. 101, no. 5, p. 53904, 2007.
- [26] L. Antognazza *et al.*, “Comparison between the behavior of HTS thin film grown on sapphire and coated conductors for fault current limiter applications,” *IEEE Trans. Appl. Supercond.*, vol. 19, no. 3, pp. 1960–1963, 2009.
- [27] C. Lacroix, J.-H. Fournier-Lupien, K. McMeekin, and F. Sirois, “Normal zone propagation velocity in 2G HTS coated conductor with high interfacial resistance,” *IEEE Trans. Appl. Supercond.*, vol. 23, no. 3, p. 4701605, 2013.
- [28] G. A. Levin, K. A. Novak, and P. N. Barnes, “The effects of superconductor–stabilizer interfacial resistance on the quench of a current-carrying coated conductor,” *Supercond. Sci. Technol.*, vol. 23, no. 1, p. 14021, 2009.
- [29] G. A. Levin, W. A. Jones, K. A. Novak, and P. N. Barnes, “The effects of superconductor–stabilizer interfacial resistance on quenching of a pancake coil made out of coated conductor,” *Supercond. Sci. Technol.*, vol. 24, no. 3, p. 35015, 2011.
- [30] T. A. Friedmann, M. W. Rabin, J. Giapintzakis, J. P. Rice, and D. M. Ginsberg, “Direct measurement of the anisotropy of the resistivity in the a-b plane of twin-free, single-crystal, superconducting YBa 2 Cu 3 O 7–  $\delta$ ,” *Phys. Rev. B*, vol. 42, no. 10, p. 6217, 1990.
- [31] J. Lu, E. S. Choi, and H. D. Zhou, “Physical properties of Hastelloy® C-276™ at cryogenic temperatures,” *J. Appl. Phys.*, vol. 103, no. 6, p. 64908, 2008.
- [32] Y. S. Touloukian and E. H. Buyco, “Thermophysical Properties of Matter (New York: IFI/Plenum),” 1970.
- [33] W. M. Haynes, *CRC handbook of chemistry and physics*. CRC press, 2014.

- [34] J. E. Gordon, R. A. Fisher, S. Kim, and N. E. Phillips, "Lattice and electronic specific heat of  $\text{YBa}_2\text{Cu}_3\text{O}_7$ ," *Phys. C Supercond. its Appl.*, vol. 162, pp. 484–485, 1989.
- [35] S. J. Hagen, Z. Z. Wang, and N. P. Ong, "Anisotropy of the thermal conductivity of  $\text{YBa}_2\text{Cu}_3\text{O}_{7-y}$ ," *Phys. Rev. B*, vol. 40, no. 13, p. 9389, 1989.